1-1-2016

Biaxial creep test study on the influence of structural anisotropy on rheological behaviour of hard rock

Chuangzhou Wu
Zhejiang University

Qingsheng Chen
National University of Singapore, qingshen@uow.edu.au

Sudip Basack
University of Wollongong, sudip@uow.edu.au

Riqing Xu
Zhejiang University

Zhenming Shi
Tongji University

Biaxial creep test study on the influence of structural anisotropy on rheological behaviour of hard rock

Abstract

Rheological characteristics are one of most important properties needed to be considered for the designing and construction for the long term stability and serviceability of underground structures in the rock mass. Up to date, although extensive studies on the rheological properties of rocks are available in the literature, most of existing studies reported the strain-time data for the axial deformation through compression rheological method and did not mention the lateral deformation, and mainly focused on the soft rocks at shallow depth. Thus, very limited attention has been paid to the rheological properties of deep and hard rock, neglecting the effects of structural anisotropy on the rheological properties. This paper presents a comprehensive in-depth study on the rheological behaviours of super-deep hard rock considering the effects of structural anisotropy by using the uniaxial and biaxial creep tests. The results revealed that significant creep behaviour can be observed in the hard rock specimens under high stress in the in-situ conditions, and the strain-time behaviour of hard rock exhibited brittle failure. The strain-time curves of hard rock exhibited two obvious phases of instantaneous creep and steady state creep without the phase of accelerated creep. Moreover, it was observed that the rheological behaviours, including the instantaneous modulus, transient creep duration, axial and lateral creep deformations, steady state creep rate, volumetric strain and contraction ratio are strongly affected by the structural anisotropy. Based on the experimental data, empirical models of the parameters governing creep behaviour have been established.

Keywords

test, rheological, influence, hard, study, creep, rock, structural, biaxial, behaviour, anisotropy

Disciplines

Engineering | Science and Technology Studies

Publication Details

Wu, C., Chen, Q., Basack, S., Xu, R. & Shi, Z. (2016). Biaxial creep test study on the influence of structural anisotropy on rheological behaviour of hard rock. Journal of Materials in Civil Engineering, 28 (10), 04016104-1-04016104-12.

Please Cite this paper as:
C.Z. Wu, Q.S. Chen, S. Basack, R.Q. Xu, and Z.M. Shi (2015) Biaxial Creep Test Study on the Influence of Structural Anisotropy on Rheological Behaviour of Hard Rock. *Journal of Materials in Civil Engineering*, ASCE DOI: 10.1061/(ASCE)MT.1943-5533.0001571.

Biaxial Creep Test Study on the Influence of Structural Anisotropy on Rheological Behaviour of Hard Rock

Chuangzhou Wu
BSc Eng (Hons.), MSc, PhD
Research Fellow
College of Civil Engineering and Architecture
Zhejiang University
866 Yuhangtang Road, Hangzhou 310058, China
Email: ark_wu@zju.edu.cn

Qingsheng Chen
BSc Eng (Hons.), MSc, PhD, P.E.
Research Fellow
Department of Civil and Environmental Engineering,
National University of Singapore,
Address: 1 Engineering Drive, E1-08-23, Singapore, 117576
Email: ceecq@nus.edu.sg

Sudip Basack
BE, MCE, PhD, MASCE, MIGS, MISRMTT, AMIEIndia, CEngIndia
Research Academic (Australian Research Council)
Centre for Geomechanics and Railway Engineering
Faculty of Engineering and Information Sciences
University of Wollongong, Wollongong City, NSW 2522, Australia.
Email: sudip@uow.edu.au

Riqing Xu
BSc Eng (Hons.), MSc, PhD
Professor
College of Civil Engineering and Architecture
Zhejiang University
866 Yuhangtang Road, Hangzhou 310058, China
Email: Xurq@zju.edu.cn

Zhenming Shi
BSc Eng (Hons.), MSc, PhD
Professor
Department of Geotechnical Engineering,
Tongji University
1239 Siping Road, Shanghai 200092, China
Email: 94026@tongji.edu.cn

Submitted To: Journal of Materials in Civil Engineering, ASCE

Biaxial Creep Test Study on the Influence of Structural Anisotropy on Rheological Behaviour of Hard Rock

Chuangzhou Wu Qingsheng Chen Sudip Basack Riqing Xu Zhenming Shi

Abstract: Rheological characteristics are one of most important properties needed to be considered for the designing and construction for the long term stability and serviceability of underground structures in the rock mass. Up to date, although extensive studies on the rheological properties of rocks are available in the literature, most of existing studies reported the strain-time data for the axial deformation through compression rheological method and did not mention the lateral deformation, and mainly focused on the soft rocks at shallow depth. Thus, very limited attention has been paid to the rheological properties of deep and hard rock, neglecting the effects of structural anisotropy on the rheological properties. This paper presents a comprehensive in-depth study on the rheological behaviours of super-deep hard rock considering the effects of structural anisotropy by using the uniaxial and biaxial creep tests. The results revealed that significant creep behaviour can be observed in the hard rock specimens under high stress in the in-situ conditions, and the strain-time behaviour of hard rock exhibited brittle failure. The strain-time curves of hard rock exhibited two obvious phases of instantaneous creep and steady state creep without the phase of accelerated creep. Moreover, it was observed that the rheological behaviours, including the instantaneous modulus, transient creep duration, axial and lateral creep deformations, steady state creep rate, volumetric strain and contraction ratio are strongly affected by the structural anisotropy. Based on the experimental data, empirical models of the parameters governing creep behaviour have been established.

CE Data Subject Headings: Anisotropy; Biaxial stresses; Creep; Laboratory tests; Rock masses; Strain rates.

INTRODUCTION

The long term load-deformation behaviour of rock, specifically denoted as *creep*, refers to the continued deformation under the effect of constant stress. The creep behaviour is one of the most important mechanical properties of rock material, since this has a major impact on the long-term stability of structures. It has been often reported that several structural failures leading to instability in rock projects were not the instances of transient destruction, but developed over time (Dusseault and Fordham, 1993; Boukharov et al., 1995; Damjanac and Fairhurst, 2010). For instance, creep failure of rock tunnels can occur after several decades of construction, and deformations in the dam foundations and abutments can last for several decades (Fan, 1993; Gudmundsson et al., 2010; Zhang et al., 2014). In view of structural safety and long-term stability of underground structures comprising of rock masses, a thorough and in-depth study on the creep behaviour of rocks is therefore of immense importance.

In the past decades, extensive laboratory investigations have been carried out on the mechanical creep behaviour of rocks (Yang et al., 1999; Maranini and Brignoli, 1999; Gasc-Barbier et al. 2004; Ma and Daemen, 2006; Yang and Jiang, 2010; Wang et al., 2014). However, most of these studies only focused on the relatively soft rocks (e.g.: rock salt, clayey rock, and tuff), as significant deformation were often observed in these rocks, thereby leading to an eventual failure. In contrast, creep in hard rock tends to be significantly less compared to the soft rock and hence it was often completely ignored (Drescher and Handley, 2003). As a result, information and literature available on the creep behaviour of hard rock is rather limited.

In the recent years, due to high demand of exploration of deep underground resources, a significant number of large-scale deep underground tunnels have been constructed in rock

mass in China. For instance, the auxiliary tunnel with length of over 16 km was constructed at a depth up to 2525 metres in the rock mass for the Jin-ping I and II Hydropower Station, where the imposed overburden stress measured was in the order of 26 - 70 MPa (Chen et al., 2015). As a result, behaviour of the rock materials become significantly complex due to high magnitudes of stress, temperature, seepage pressure and rock burst, thereby bringing about a series of new challenges for rock mechanics and engineering (Meng et al., 2006; Qian and Li, 2008; Zhou et al., 2010). The observed field data revealed that, pronounced creep strains occurred in the hard rocks in these deep underground structures, adversely affecting the long-term structural stability (Liu et al., 2013; Zhou et al, 2005; Zhou et al., 2010).

Over the past few decades, structural anisotropy has attracted considerable interest in the field of rock mechanics and engineering, as it is one of the most important factors affecting the strength and deformation characteristics of rocks. (McLamore and Gray, 1967; Amadei, 1996; Chen et al., 1998; Ghazvinian et al., 2013; Noorian Bidgoli and Jing, 2014). Till date, most of the existing studies have extensively investigated the effects of anisotropy on the elasto-plastic properties (viz., modulus of elasticity, compressive strength and failure strength) of rocks. However, very limited attentions have been paid to the effect of anisotropy on the rheological behaviour of rocks (Weijermars, 1992; Dubey and Gairola, 2000, 2008; Zhang et al, 2009). In addition, even though various creep test data on the shallow depth soft rocks have been available in the literature, most of them are based on uniaxial compression creep results, without any information on the possible lateral deformation (Maranini and Brignoli, 1999; Gasc-Barbier et al. 2004; Ma and Daemen, 2006; Yang and Jiang, 2010; Wang et al., 2014). Therefore, investigation on the effects of structural anisotropy on the rheological properties of rocks, including both axial and lateral deformations, is of immense importance for appropriate design and construction of underground structures in anisotropic rock mass, especially for large-scale deep underground projects.

In this study, the main objective is to investigate the rheological behaviours of super-deep hard rock considering the effects of structural anisotropy by using the uniaxial and biaxial creep tests. A series of uniaxial and biaxial creep tests with multiple step loading were performed out on the rock specimens with different structural anisotropy (inclination of bedding plane). The effects of structural anisotropy on the rheological behaviours, including the instantaneous modulus, transient creep duration, axial and lateral creep deformations, steady state creep rate, volumetric strain and contraction ratio of the rocks have been studied in details.

PROJECT DESCRIPTION

The project under the purview of the present study is the Jinping II hydropower station, located on the Great Jinping River Bend of Yalong River, Sichuan Province in South-western part of China (see Figure 1). It consists of a 310 m high natural drop created by the Jinping Yalong river bend which diverts the water to headrace tunnels travelling through Jinping Mountain. The hydropower station is expected to have an installed capacity of 4.8 GW and an annual power generation of 24.2 TWh (East China Hydropower Investigation & Design and Research Institute, 2005). The site involved exploration of 7 parallel tunnels, with the length of a single tunnel of approximately 16.7 km, majority (about 75%) of which is being covered by rock mass having thickness and maximum depth over 1500 m and 2525 m respectively. The in-situ earth stress measured in the rock mass was in the order of 26 - 70 MPa and the maximum water pressure was 10 MPa (Chen et al. 2015). The surrounding rock in the hydropower station mainly consists of marble, slate, chlorite schist, and metamorphic sandstone, which belong to hard rock in the Middle and Upper series of the Triassic (Shan and Yan, 2010). The geological profile of the rock mass in the project site is shown in Figure 2.

The natural dip angle of the in-situ rock bed was 88^0, thus the bedding planes were almost vertical. The actual stress condition in the rock mass in the vicinity of the tunnel surface is complex (Cai 2008). It is an established finding that tunnel construction induces differential settlement of the ground surface (Chow 1994; Fattah *et al.* 2011; Hesami *et al.* 2013), with maximum settlement occurring over the tunnel centerline and gradually diminishing with distance. Such differential settlement induced a shear stress component in the rock mass as well. Fig.2(b) demonstrates the stress components induced at a certain point '*A'* of the rock mass adjacent to the tunnel. Due to the complex nature of the induced stresses coupled with nonlinear variation of stress-strain under creep loading, it is difficult to accurately determine the exact orientation of maximum shear stress and requires enormous analytical or computational effort. To simplify, the creep behavior of the hard rock mass has been studied, based on laboratory experimentations with biaxial stresses being applied on rock specimen parallel and perpendicular to the in-situ bedding planes. The failure of hard rock under major principal stress applied parallel to the bedding planes is initiated by the combination of shearing and seperation of bedding planes, leading to higher creep strain and aparently showing higher modulus compared to that of hard rock sample under major principal stress applied perpendicular with the bedding planes, where the failure is caused by the combination of shearing and compression of beding planes (Bosmon *et al.* 2000; Dubey and Gairola, 2008; Zhang *et al.* 2015a).

LABORATORY INVESTIGATIONS

Due to the high in-situ stress in the rock mass, significant creep deformation of rock mass is expected in the field. Also, the observed anisotropic properties associated in the bedding planes necessitated an in-depth study on its creep properties aided with the influence of structural anisotropy (Shan and Yan, 2010; Wu et al., 2010). The details of the uniaxial and biaxial laboratory tests performed are described below.

Sample Preparation

The *Greenschist* specimens were sampled from the auxiliary tunnel of the hydropower station (Figure 3(a)) at a depth of 1600 m in the rock mass, where the maximum geostress was measured 42 MPa. Greenschist strata exhibit well developed bedding having white marble bands and lens (Figure 3(b)), with the strike and the dip angles as about 296°and 88° respectively. The uniaxial compressive strength of the Greenschist rock samples usually varies in the range of 40 – 68 MPa under dry condition (Chen et al. 2015).

The test program reported in this paper involves rock mass to be quarried from significant depth and cutting them to desired shapes which is a difficult task. In this study, it is noted that the size effect on the creep properties of rock is not considered. Rock samples in the shape of cube of dimensions of 10×10×10 cm^3 (Figure 3(d)) were prepared with the help of rock cutting machine (Figure 3(c)). In the field, the in-situ overburden stress in the rock strata is likely to alter in reality, for example during construction of superstructure on the ground surface, excavation, etc.. Thus, for the creep tests, application of sustained loading in several steps is close to the field conditions. Such multiple step loading has also been imparted in laboratory creep tests by many other researchers (Eslami *et al.* 2012; Wang *et al.* 2015; Zhang *et al.* 2015b). To investigate the effects of structural anisotropy on the rheological behaviours of hard rock, three *sets* of specimens under multiple-step loading with different combination of loading directions were used for the tests, as discussed later in details. In these tests, however, the bedding plane orientation with respect to the stress direction have been denoted as: UN, UP, BNP, BPN and BPP, where, the first letter indicates the nature of test conducted ('U' for uniaxial and 'B' for biaxial modes), while the second and third letters denote the orientation of bedding plane with respect the applied major and minor principal stresses (σ_1 and σ_2) respectively ('P' for parallel and 'N' for normal).

Test Set Up and Methodology

Uniaxial and biaxial compression creep tests were performed with the close-loop servo-controlled CSS-1950 Biaxial Rheological testing machine (Figure 4) at Tongji University, China. During the tests, vertical and horizontal forces were applied on the rock specimen simultaneously or separately, and the corresponding deformations were recorded with the automated data logger. The capacities of this machine were: 500 kN and 250 kN in vertical compression and extension respectively, while 300 kN in horizontal compression. The measurement of deformation was controlled by a set of Linearly Variable Differential Transducers (LVDT) with the accuracy in the range of ±0.0001 mm.

In this study, creep tests with multiple step loadings were carried out by starting with a relatively lower stress level and increasing in steps, allowing a certain rest period in each such steps to allow for creep deformation. When the strain rate became lower than 0.01 mm/day, the creep deformation was considered to be stabilized and the subsequent stress-step was applied. During the tests, few specimens were observed to fail instantaneously at higher stress levels. All the creep tests were performed under controlled temperature condition at 30^{o}C. The test program in this study is summarized in Table 1.

EXPERIMENTAL RESULTS: ANALYSES AND INTERPRETATIONS

The observed data from the uniaxial and biaxial creep tests have been analysed and interpreted to arrive at specific conclusions, as discussed herein. The appropriate values of strains relevant to instantaneous, transient and steady-state creep increments under the uniaxial and biaxial tests are summarized in the Table 2. It is observed that the values of strains relevant to instantaneous, transient and steady state creep vary from 0.594-1.1, 0.0056-0.086 and 0.0064-.048 under uniaxial loading, while 0.24-3.557, .0197-0.3 and 0.0223-0.313 under biaxial loading respectively.

Strain-Time Response

Uniaxial Compression

Figure 5 (a) presents the strain-time curves of rock specimens under uniaxial compression creep tests (UP and UN). Since the measured in-situ earth pressure was 42 MPa, the maximum value of the major principal stress σ_1 for these uniaxial creep tests were kept conveniently at 40 MPa, and the stress in the creep test have been increased in 4 equal steps. For each step, the deformation was observed to increase in a sudden manner immediately after the application of the load and thereafter stabilized gradually (see Figure 5 (b)). For both specimens, it is observed that the magnitude of instantaneous creep increment progressively decreased at each of the stress steps. For instance, the instantaneous increment of creep strain was 1.3 x 10^{-3} for an increase in stress step (σ_1) from 0-10 MPa, while the same have been recorded as 0.74 x 10^{-3}, 0.7 x 10^{-3} and 0.64 x 10^{-3} for the stress steps of 10–20 MPa, 20-30 MPa and 30-40 MPa, respectively. This may be attributed to the possible strain hardening of the rock specimen during the loading process. It may be noted that such observation is opposite to those for soft rocks (Gasc-Barbier et al., 2004; Zhang et al. 2013). Also, compared with the typical creep behaviour observed in soft rocks (Dubey and Gairola, 2008), no accelerated creep was observed in the hard rock specimen after steady state creep, but a subsequent brittle failure was observed at higher stress levels.

By comparing the test results for UP and UN, it is clear that the strain-time behaviour of rock specimen was strongly affected by the structural anisotropy. The creep strain for specimen compressed normal to bedding plane (UN) was much less compared to those compressed parallel to bedding (UP) for each loading step. This may be justified by the fact that the larger creep developed in UP in comparison with UN is caused by induced tensile stress acting perpendicular to the bedding planes and is attributed by least strength in tensile stress

environment (Lama and Vutukuri, 1978; Dubey and Gairola, 2008). That is, for compression parallel to the bedding planes, larger creep deformation is expected due to the possible relative slippage between the planes, compared to the case where the applied stress is normal to the bedding planes (Lama and Vutukuri, 1978; Dubey and Gairola, 2008). The UN specimen deformed perpendicular to bedding plane showed smaller creep strain is possibly due to alignment of bedding plane in the direction of least induced tensile and shear stresses.

Biaxial Compression

Figure 6 presents the strain-time curves of the specimens with different combinations of bedding plane inclination and loading pattern (i.e. BNP, BPN, and BPP). For comparison with uniaxial creep test results, the maximum value of the major principal stress σ_1 for these biaxial creep tests were kept conveniently at 40 MPa, with the stress ratio σ_2 / σ_1 kept at 0.5. For all the tests, both the axial as well as lateral strains were measured. It is noted that the in-situ vertical and horizontal stress components induced in the rock mass in the large-scale deep underground tunnels under consideration here were measured as 26-70 MPa and 10-40 MPa respectively (Chen *et al.* 2015), with the stress ratio σ_2 / σ_1 varying in the range of 0.38 – 0.57, the average value being 0.48. Also, the Authors would like to point out that in the laboratory, performing one biaxial creep test took a long time, sometimes up to as high as 12 days. Also, it is very difficult to quarry hard rock mass from a significantly great depth below the ground surface ($z \approx 1.6$ km). The effort required to cut the collected rock mass to specimens of regular size (10 cm^3) is enormous. Thus, for the laboratory experimentations, the value of 0.5 for the stress ratio σ_2 / σ_1 in the biaxial tests was chosen.

As in case of uniaxial loading, the creep deformation at each stress step was observed to increase suddenly manner after load application followed by a gradual stabilization. Also, increase in the instantaneous creep strains in both axial and lateral directions was also found to progressively decrease with increasing stress steps. As the applied stress σ_1 varied in the

range of 10 - 40 MPa, the maximum axial creep strain was observed to increase in the ranges of 0.0009 – 0.0019, 0.0016 – 0.0027 and 0.0037 – 0.0069 in case of BPN, BNP and BPP respectively, while the corresponding lateral creep strain was observed to increase in the ranges of 0.00095 – 0.0016, 0.0011 – 0.0019, 0.0014 – 0.0023, respectively. That is, in both axial and lateral directions, the creep strains in the BPP specimen showed maximum creep deformations whereas the BNP specimen showed minimum creep strain (Figure 6). This can be justified by the fact that in case of the principal stresses (σ_1 and σ_2) being parallel to the bedding planes, the creep deformation is associated with separation of the planes initiating greater deformation compared to the cases where bedding plane is normal to the major principal stress, inducing maximum restraint to the deformations (Dubey and Gairola, 2008). Additionally, it was found that the development of lateral creep strain was also significantly affected by the structural anisotropy of the specimens under same stress levels. The results showed that the axial creep strain was close to lateral creep strain at low stress level ($\sigma_1 < 20$MPa) for BNP, whereas significant difference between axial and lateral creep strains can be observed in the BPN and BPP specimens, especially at high stress level ($\sigma_1 = 40$MPa). This may be attributed to the maximum compressive stress acting normal to the bedding planes in BNP in comparison with the counterparts for BPN and BPP specimens, thereby resulting in less relative creep deformation among bedding planes and smaller discrepancy between lateral and axial creep strains. Besides, from Fig. 5(a), it was observed that for uniaxial loading, brittle failure took place at peak stress level ($\sigma_1 = 40$ MPa). On the contrary, for biaxial loading (see Fig. 6), no such failure is observed at the same stress level ($\sigma_1 = 40$ MPa). This highlights that the strength of rock specimens was significantly improved by the application of minor principal stress, which implies that the existing knowledge about the creep behaviour of rocks obtained from uniaxial creep tests cannot be directly applied for the cases for biaxial compression conditions. Thus, the creep behaviour of hard rock has been

found to be affected strongly by its structural anisotropy as well as the stress conditions, which is studied in more details below.

Effect of Structural Anisotropy

Instantaneous Modulus

Instantaneous modulus is one of the most important parameters governing the rheological properties of rocks. In this study, the instantaneous modulus E_i has been defined as the ratio of major principal stress σ_1 to the instantaneous creep strain ε_i (see Figure 7). The variation of E_i with σ_1 using the uniaxial and biaxial creep test data are shown in Figure 8. It is observed that the instantaneous modulus E_i for the specimens under biaxial compression stresses (BNP, BPN and BPP) were significantly higher than the counterparts for the specimens under uniaxial compression stresses (UP and UN), especially at high stress levels (σ_2>20MPa). This is closely consistent with the observations in creep strains discussed earlier where the creep strain was found to be much smaller for the BPN, BNP and BPP specimens compared to the counterparts of UP and UN specimens. Interestingly, based on the experimental data, it was found that two increasing pattern of E_i with σ_1 were observed. As observed from the Figure 8(a), for the test conditions BNP, BPN and UN, the best fit curves, with the value of R^2 above 0.96, have been parabolic with ascending slope and satisfy the following Equation:

$$E_i = K\sigma_1^m \quad \ldots(1)$$

For the test series BPP and UP (see Figure 8(b)), on the other hand, the regression curves are observed to be parabolic with descending slope, with the following Equation:

$$E_i = K_1\sigma_1^2 + K_2\sigma_1 + K_3 \quad \ldots(2)$$

The values of the constants K, m, K_1, K_2 and K_3 have been given in the respective Figures. These observations may be justified by the fact that, for BNP, BPN and UN conditions, the

hardening occurred with the increasing applied stress levels, while for BPP and UP conditions, hardening occurred mainly at low stress level (σ_1 <20MPa) but it diminished with increasing σ_1 due to the progressive separation of bedding planes caused by increasing tensile stress induced normally on the bedding planes. That is, whenever both the applied principal stresses are oriented along the bedding planes (Fig. 8(b)), relative slippage between the bedding planes possibly induces larger creep deformation with reduced values of E_i. On the contrary, with at least one of the applied principal stresses being normal to the bedding planes (Fig. 8(a)), the resistance to creep deformation is likely to increase, which initiates increase in the value of E_i.

Steady State Creep Rate

The steady state creep rate 휀̇has been defined as the ratio of the steady state creep strain ε_s to the steady state creep duration T_s (see Figure 7). Figure 9 presented the variation of 휀̇with σ_1 obtained from the uniaxial and biaxial creep test data, respectively. It is clear that the steady state creep rate 휀̇of the specimens under uniaxial compression stresses, especially for case of UP, were significantly higher than the biaxial compression stresses (BPN, BNP, and BPP). As discussed earlier, these may attributed to the facts that, compared with the specimens under biaxial compression conditions, no additional restraints existed in the specimens under uniaxial compression, thereby inducing greater tensile stress perpendicular to bedding planes with a result of accelerating the development of creep strains in specimens under uniaxial compression stress condition, especially in UP specimen. These explanations can also be further justified by the experimental observations for BPP and UP specimens, where less resistance to the separation and sliding among/along the bedding planes compared the BPN, BNP and UN specimens, resulting that the steady state creep rate 휀̇of specimens BPP and UP were much higher than those of BNP, BPN and UN, respectively. This indicated that the

structural anisotropy as well as the applied stress conditions play significant role in the creep behaviours of rocks. Additionally, it is of great interest that different development models of 휀̇with σ_1 were found between the specimens under biaxial and uniaxial compression stresses. As may be noted from the Figure 9(a), for the biaxial creep tests (BNP, BPN and BPP), the best fit curves, with the value of R^2 above 0.95, have been parabolic with the slope initially descending to a minimum value of 휀̇and thereafter ascending gradually. These curves are found to satisfy the following Equation:

$$휀̇= 퐴_1휎_1^2 + 퐴_2휎_1 + 퐴_3 \quad \ldots(3)$$

For the uniaxial creep tests (UN and UP), on the other hand, the regression curves, having the R^2 values above 0.96, are observed to be parabolic with ascending slopes (see Figure 9(b)), with the following Equation:

$$휀̇= 퐶_1휎_1^2 + 퐶_2휎_1 + 퐶_3 \quad \ldots(4)$$

The values of the constants C_1, C_2 , C_3 , A_1, A_2 and A_3 have been given in the respective Figures. The above observations can be attributed to the fact that, for the specimens under biaxial compression stresses, hardening induced by compression was greater than the softening caused by the induced damage (opening of the minor cracks) in the specimens at low stress level (σ_1 <20MPa) due to the restraints of lateral deformations, but this trend reversed when the specimens were subjected to higher stress levels beyond 20 MPa. That is, in biaxial creep tests, application of confining stress σ_2 is likely to introduce resistance to creep deformation. At lower stress levels (10 MPa $\leq \sigma_1 \leq$ 20 MPa), such resistance possibly retards the creep deformations compared to higher stress levels ($\sigma_1 \geq$ 20 MPa). In contrast, for the specimens under uniaxial compression stresses, no lateral restraints existed in the specimens, thereby resulting in that the damage induced softening was stronger than the compression induced hardening in the specimens under all stress levels.

This justifies the instantaneous decrease in the value of $\dot{\varepsilon}_{ss}$ at lower stress level in case of biaxial loading (see Fig. 9(a)), in contrary to the uniaxial loading (see Fig. 9(b)). These further highlight that the existing knowledge about creep behaviours of rocks obtained from uniaxial compression creep tests cannot be applicable for the cases of biaxial compression stress conditions.

Transient Creep Duration

The variation of the transient creep duration t_{tr} defined in Figure 7 has been studied against the major principal stress σ_1. It can be observed that, for the BNP, BPN and BPP specimens, the time duration of transient creep phase showed pronounced variations, where the slope of the curve is the highest negative in the case of BPN (-0.30) and the least negative in the case of BNP (-0.09). This implies that the structural anisotropy played a significant role in the duration of transient creep phase for the specimens under biaxial compressions stresses, especially at the low stress level (σ_1<20MPa) where the duration of transient creep phase for BPN is the longest, while the duration of transient creep phase for BNP is the shortest. This can be due to that, the transient creep developed in BPN was attributed by smooth opening of inherent cracks, pore spaces and voids lying along bedding planes in induced tensile stress acting perpendicular to bedding plane (favourable for opening of cracks and voids), while the transient creep developed in BNP was due to attributes of opening of inherent cracks, pore spaces and voids lying parallel to beddings, and respond minimally to unfavourably oriented induced tensile stress acting parallel to bedding planes (Dubey and Gairola, 2008). Also, it is clear that, as the stress level increased, the time duration of transient creep phase showed a linearly decreasing trend and the curves were converging, indicating that the effect of structural anisotropy on duration of transient creep phase decreased linearly with increasing stress level. By comparison, for the specimens UN and UP, much smaller variation in the time duration of transient creep against applied stress levels can be observed, where the

slopes of the curves are -0.44 and -0.42, respectively. That is, the effect of structural anisotropy on the duration of transient creep phase for the specimen under uniaxial compression stresses can be negligible. Besides, it is observed that, compared with BPN, BNP and BPP specimens, the duration of transient creep phases for UN and UP decreased more quickly with the increasing stress levels. As observed (see Figure 10), the parameter T_t decreases fairly linearly with increasing σ_1 (R^2 > 0.96 and 0.93 for biaxial and uniaxial conditions respectively). The Equation of the best fit lines has been in the following form:

$$T_t = L_1 \sigma_1 + L_2 \quad \ldots(5)$$

The values of the constants L_1 and L_2 have been given in the Figure 10.

Volumetric Strain and Contraction Ratio

In case of biaxial creep tests, the measured axial and lateral creep strain data have been utilized to calculate the volumetric creep strains developed and the contraction ratio have been obtained as well. From the theory of Plasticity (Chakrabarty, 2006), the contraction ratio η, have been defined as the lateral to axial strains developed in an elasto-plastic solid body. The time pattern of variation of these two parameters has been studied.

As observed from Figure 11(a), the parameter was found to gradually increase stepwise in each of the stress-steps in the ranges of 0.003 – 0.005, 0.004 – 0.007 and 0.0068 – 0.0115 for the test conditions relevant to BNP, BPN and BPP respectively. As mentioned earlier, with the loading directions being parallel to the bedding planes, the axial and lateral strains produced have been greater, which attributed to a greater magnitude of the volumetric strain as well. The parameter η, on the other hand, was found to vary between 1.15 – 0.73, 0.7 – 0.8 and 0.36 – 0.44 for the tests denoted as BNP, BPN and BPP respectively (see Figure 11(b)). Interestingly, this observation contradicts the theory of plasticity ($\eta \leq 0.5$) which may be

justified by the fact that the conventional plasticity theory is valid for elasto-plastic bodies under gradually applied stresses whereas the current tests deal with sustained stress under uniaxial and biaxial condition; the induced strains and the calculated contraction ratio are therefore essentially time dependent. The contraction ratio of a material is defined as the ratio of its lateral to longitudinal strain under inelastic condition (Chakraborty 2006). Whenever major principal stress is applied normal to the bedding plane, more lateral creep strain is induced compared to the longitudinal strain, due to possible relative slippage between the bedding planes. With increase in magnitude of the applied major principal stress in each loading step, such slippage progressively increases. Thus, for BNP, a significant decrease in the magnitude of contraction ratio was observed with increase in each of the loading steps.

CONCLUSIONS

Creep behaviour of hard rock and the influence of its structural anisotropy is a study area of immense importance, especially for civil engineering projects involving long and deep underground tunnels to be constructed through hard rocks. To understand the influence of structural anisotropy on rheological behaviour of hard rock, an extensive series of laboratory creep tests have been performed with Greenschist rock samples quarried from a hydropower project. The tests involved application of sustained stresses under uniaxial and biaxial conditions in several steps and measuring the resulting creep deformation.

The study indicated that in each step loading, the deformation increased suddenly after the immediate application of load and thereafter stabilized gradually. No component of accelerated creep has been noticed. The magnitude of instantaneous creep increment progressively decreased in each of the stress steps from 0.0074 to 0.0064 under uniaxial loading condition, with stress level increasing from 10-40 MPa.

At any specific stress level, creep deformations are higher for the loading conditions parallel to the bedding planes compared to those observed for the normal loading cases. The orientation of bedding plane compared to loading direction also affects the magnitude and extent of lateral deformation produced.

While a brittle failure was observed at high stress level (σ_1 =40MPa) under uniaxial loading condition, no such failure did occur for biaxial loading condition under identical stress level. This highlights significant improvement in the rock strength by the application of minor principal stress.

Higher steady state creep rate (휀̇) was observed for BPP and UP compared to BNP, BPN and UN. This eventually highlights the fact that a hard rock is stronger when the loading is normal to bedding plane. Also, under biaxial stress condition, the parameter 휀̇initially decreases with the increasing magnitude of σ_1 and subsequently increases after a minimum value of 휀̇is attained. In case of uniaxial loading, on the other hand, a steady increasing trend is noted.

From the regression analysis conducted with the test data, the instantaneous modulus E_i, steady state creep rate 휀̇and transient creep duration T_t were found to be appropriate functions of the applied major principal stress σ_1. For σ_1, the parameter E_i was found to vary in a parabolic manner with the stress σ_1, the slopes being ascending for loading normal to the rock bedding planes, while descending slopes for loading condition parallel to bedding planes. The steady state creep rate 휀̇was also found to vary parabolically with σ_1. With increasing σ_1, the transient creep duration T_t was found to decrease linearly. In case of biaxial loading condition, the lines were observed to converge as the magnitude of σ_1 increases, while no such convergence was observed in case of uniaxial loading. This indicates that the

orientation of bedding planes plays a significant role on the transient creep duration for biaxial condition only.

In case of biaxial stress tests, the measured volumetric strains 휀볼was found to increase stepwise in each stress-steps. The calculated contraction ratio η was observed to vary from 0.44 to 1.15 under the applied stress levels.

ACKNOWLEDGEMENT

This work was financially supported by National Natural Science Foundation of China (Grant No: 51178420; 51509219)

NOTATION LIST

σ_1, σ_2 = the applied major and minor principal stress, respectively (MPa);
UN = uniaxial test normal to bedding plane;
UP = uniaxial test parallel to bedding plane;
BNP = biaxial test with major and minor principal stresses normal and parallel to bedding plane respectively;
BPN = biaxial test with major and minor principal stresses parallel and normal to bedding plane respectively;
BPP = biaxial test with major and minor principal stresses parallel l to bedding plane;
E_i = instantaneous modulus (GPa);
ε_i = the instantaneous creep strain;
K, m, K_1, K_2 and K_3 = regression constants for instantaneous modulus;
휀̇ = the steady state creep rate (10^{-3}/hour);
T_s = the steady state creep duration (hours)
C_1, C_2 , C_3 , A_1, A_2 and A_3 = regression constants for the steady state creep rate;
휀̇ − the transient creep duration (hours);
L_1 , L_2 = regression constants for the transient creep duration;
휀 = the volumetric creep strain;
η = contraction ratio.

REFERENCES

Amadei, B. (1996) Importance of anisotropy when estimating and measuring in situ stress in rock. International Journal of Rock Mechanics and Mining Sciences, 33(3), 293-325.

Bosmon, J. D., Malan, D. F. and Drescher, K. (2000). Time-dependent tunnel deformation at Hartebeestfontein Mine. *J. South African Inst. Mining and Metallurgy*, October 2000, 333-340.

Boukharov G.N., Chanda M.W., Boukharov, N.G., (1995). The three progresses of brittle crystalline rock creep. International Journal of Rock Mechanics and Mining Sciences.32(4), 325-335

Cai, M. (2008). Influence of intermediate principal stress on rock fracturing and strength near excavation boundaries - insight from numerical modeling. *Int. J. Rock Mech. Min. Sci.* 45(5), 763–772.

Chakrabarty, J. (2006). Theory of Plasticity. Elsevier/Butterworth-Heinemann

Chen, B.R., Feng, X.T., Li, Q.P., Luo, R.Z., and Li, S.J. (2015) Rock burst intensity classification based on the radiated energy with damage intensity at Jingpin II hydropower station, China. Rock mechanics and Rock Engineering, *48*(1), 289-303

Chen, C.S., Pan, E., and Amadei, B. (1998) Determination of deformability and tensile strength of anisotropic rock using Brazilian tests. Journal of Rock Mechanics and Geotecnical Engineering 35(1), 43-61

Chow, L. (1994). The prediction of surface settlements due to tunneling in soft ground, *M.Sc. thesis*, Brasenose College, University of Oxford, UK.

Damjanac, B., Fairhurst, C. (2010). Evidence for a long-term strength threshold in crystalline rock. Rock Mechanics and Rock Engineering, 43(5), 513-531

Drescher, K., and Handley, M.F. (2003) Aspects of time-dependent deformation in hard rock at great depth. The Journal of The South African Istitute of Mining and Metallurgy, 103:325–335

Dubey, R.K., Gairola, V.K., (2000) Influence of structural anisotropy on uniaxial compressive strength of pre-fatigued rocksalt from Himachal Pradesh, India. International Journal of Rock Mechanics and Mining Sciences. 37(6), 993-999

Dubey, R.K., Gairola, V.K., (2008) Influence of structural anisotropy on creep of rocksalt from Simla Himalaya, India: An experimental approach_.Journal of Structural Geology, 30(6), 710-718

Dusseault, M.B., Fordham, C.J., (1993) Time dependent behaviour of rocks. In: Comprehensive Rock Engineering: Principles, Practice and Projects. Pergamon Press. Oxford, 119-149

East China Hydropower Investigation & Design and Research Institute (2005) The feasibility Report of Jinping II Hydropower Project, Hangzhou, China

Elsami, J., Hoxha, D and Grgic, D. (2012). Estimation of the damage of a porous limestone using continuous wave velocity measurements dring uniaxial creep tests, *Mechanics of Materials*, 49 (2012), 51-65.

Fan, G.Q., (1993) Rheological Mechanics of Geotechnical Engineering. China Coal Industry Publishing House, Beijing, China

Fattah, M. Y., Slash, K. T. and Salim, N. M. (2011). Settlement trough due to tunneling incohesive ground. *Indian Geotechnical Journal*, 41(2), 2011, 64-75.

Gasc-Barbier, M., Chanchole, S., Bérest, P. (2004) Creep behaviour of bure clayey rock. Applied Clay Science, 26, 449-458

Ghazvinian, A., Geranmayeh Vaneghi R., Hadei, M.R., and Azinfar, M.J. (2013) Shear behavior of inherently anisotropic rocks, International Journal of Rock Mechanics and Mining Sciences, 61, 96-110

Gudmundsson, A., Simmenes, T.H., Belinda, L., Sonja, L.P., (2010). Effects of internal structure and local stresses on fracture propagation, deflection, and arrest in fault zones, Journal of Structural Geology, 32(11), 1643-1655

Hesami, S., Ahmadi, S.,Ghalesari, A. T. and Hasanzadeh, A. (2013). Ground surface settlement prediction in urban areas due to tunnel excavation by the NATM, *Elec. J. Geotech. Engrg.*, 18 (J), http://www.ejge.com/2013/Ppr2013.189alr.pdf

Lama, R.D., and Vutukuri, V.S. (1978). Handbook on Mechanical Properties of Rocks. Vol III. Trans Tech Publications. pp. 209-323, pp. 383-388

Liu L., Wang G.M., Chen J.H. and Yang S. (2013) Creep experiment and rheological model of deep saturated rock. Transactions of Nonferrous Metals Society of China, 23(2), 478-483

Lobo-Guerrero, S. and Vallejo, L. (2006). Application of Weibull statistics to the tensile strength of rock aggregates. *Geotech. Geoenviron. Engrg.*, 132 (6), 786-790.

Ma, L., Daemen, J. J.K. (2006) An experimental study on creep of welded tuff. International Journal of Rock Mechanics and Mining Science, 43(2):282-291

Maranini, E., Brignoli, M. (1999) Creep behaviour of a weak rock: experimental characterization. International Journal of Rock Mechanics and Mining Science,36(1):127-138

Massonet, C., Olszac, W. and Philips, A. (2014). *Plasticity in structural engineering, fundamentals and applications*, Springer-Verlag Wein GMBH.

McDowell, G. R., and Amon, A. (2000). The application of Weibull statistics to the fracture of soil particles. *Soils Found.*, 40 (5), 133–141.

McLamore, R., Gray, K.E., (1967)The mechanical behaviour of anisotropic sedimentary rocks. Journal of Engineering for Industry, 89(1), 62-73

Meng, Z.P., Li M.S., and Lu, P.Q., Tian, J.Q. and Lei, Y. (2006) Temperature and pressure under deep conditions and their influences on mechanical properties of sandstone[J]. Chinese Journal of Rock Mechanics and Engineering, 25 (6), 1177-1181

Noorian Bidgoli, M., and Jing, L. (2014) Anisotropy of strength and deformability of fractured rocks, Journal of Rock Mechanics and Geotecnical Engineering, 6, 156-164

Qian, Q.H., and Li, S.C. (2008) A review of research on zonal disintegration phenomenon in deep rock mass engineering. Chinese Journal of Rock Mechanics and Engineering, 27(6), 1278-1284

Shan, Z.G., and Yan, P. (2010) Management of rock bursts during excavation of the deep tunnels in Jinping II Hydropower Station. Bulletin of Engineering Geology and the Environment, 69,353-363

Tomanović, Z. (2012). The stress and time dependent behaviour of soft rocks, Građevinar, 64 (2012) 12, 993-1007 993.

Wang, G.J., Zhang, L., Zhang, Y.W., and Ding G.S. (2014) Experimental investigations of the creep–damage–rupture behaviour of rock salt. International Journal of Rock Mechanics and Mining Sciences, 66,181-187

Wang, W., Cao, Y., Zhu, Q., Xu, W. and Shao, J. (2015). Experimental investigation and constitutive modelling of creep-damage behaviours in monzogranite, *J. Environ. Civil Engrg.*, 19 (S1), 54-69.

Weijermars, R. (1992). Progressive deformation in anisotropic rocks. Journal of Structural Geology, 14(6), 723-742

Wu, S.Y., Shen, M. B., and Wang J. (2010) Jinping Hydropower Project: main technical issues on engineering geology and rock mechanics, Bulletin of Engineering Geology and the Environment, 69,325-332

Yang, C.H., Daemen, J.J.K., and Yin, J.H. (1999) Experimental investigation of creep behaviour of salt rock. International Journal of Rock Mechanics and Mining Science, 36(2), 233-242

Yang, S.Q. and Jiang, Y.Z. (2010) Triaxial mechanical creep behaviour of sandstone. Mining Science and Technology, 20 (3), 339-349

Zhang X.G., Ma G.W., Wu W., Yan L., Li M.Y., and Chen, Q.S. (2009) An Analysis of Model Tests on Rock Cavern Damage Induced by Underground Explosion. 9th International Conference on Analysis of Discontinuous Deformation (ICADD9), 2009/11/25-2009/11/27, pp625-632, Singapore. DOI: 10.3850/9789810844554-0133

Zhang, Y., Xu, W., Shao, J., Zhao, H. and Wang, W. (2015a). Experimental investigation of creep behavior of clastic rock in Xiangjiaba Hydropower Project, *Water Science & Engineering*, 8 (1), 55-62.

Zhang, Y., Xu W.Y., Gu, J.J., and Wang W. (2013). Triaxial creep tests of weak sandstone from fracture zone of high dam foundation. Journal of Central South University, 20, 2058-2536

Zhang,Y., Shao J.F., Xu W.Y., Zhao H.B., and Wang W., (2015b). Experimental and numerical investigations on strength and deformation behaviour of cataclastic sandstone, Rock Mechanics and Rock Engineering, 48(3), 1083-1096

Zhou, H.W., Xie, H.P., Zuo, J.P. (2005) Developments in researches on mechanical behaviours of rocks under the condition of high ground pressure in the depths, Advances in Mechanics, 35 (1): 91-99.

Zhou, H.W., Xie, H.P., Zuo, J.P., Du, S.H., Man, K., Yan, C.Y. (2010). Experimental study of the effect of depth on mechanical parameters of rock. Chinese Science Bulletin, 2010, 55(34): 3276-3284.

TABLE AND FIGURE LIST

Table List

Figure List

Table 1 Summary of Test Program in this study						
Loading Type		σ_2/σ_1	Step Loading σ_1 (MPa)			
			First step loading	Second step loading	Third step loading	Fourth step loading
Uniaxial compression	UN, UP	0	10	20	30	40
Biaxial compression	BNP, BPN, BPP	0.5				

Table 2 Summary of strains for instantaneous, transient and steady-state creep increments under uniaxial and biaxial stresses

Loading type		Step Loading σ_1 (MPa)	Instantaneous creep (10^{-3})	Transient creep (10^{-3})	Steady-state creep (10^{-3})
Uniaxial compression	UN	10	1100.0	5.6	6.4
		20	639.0	14.0	12.0
		30	623.0	47.6	34.4
		40	594.0	50.0	48.0
	UP	10	1276.0	6.0	12.0
		20	760.0	10.0	14.0
		30	631.0	16.0	18.0
		40	619.0	12.0	30.0
Biaxial compression	BNP	10	851.0	43.3	71.8
		20	387.0	47.5	51.5
		30	240.0	19.7	22.3
		40	112.0	66.0	84.0
	BPN	10	1531.0	61.2	59.7
		20	285.0	18.5	26.6
		30	269.0	55.0	76.0
		40	258.0	288.0	152.0
	BPP	10	3557.0	100.3	127.7
		20	920.0	69.8	85.3
		30	488.0	165.9	187.1
		40	502.0	300.9	313.1

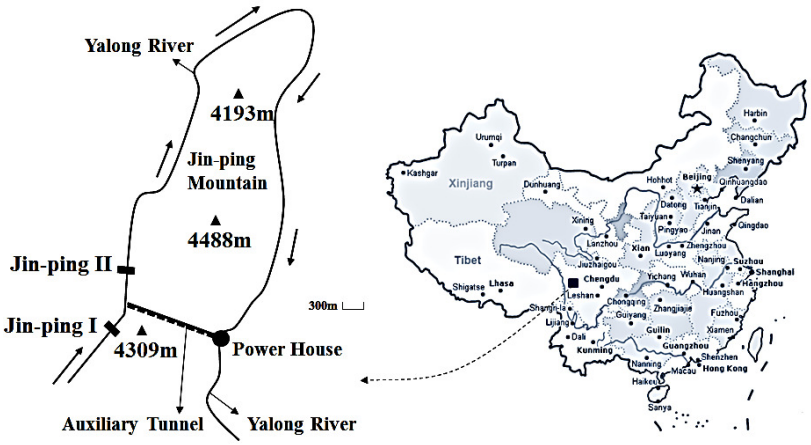

Figure 1: Location of the Jin-ping I and II Hydropower stations at Sichuan, China

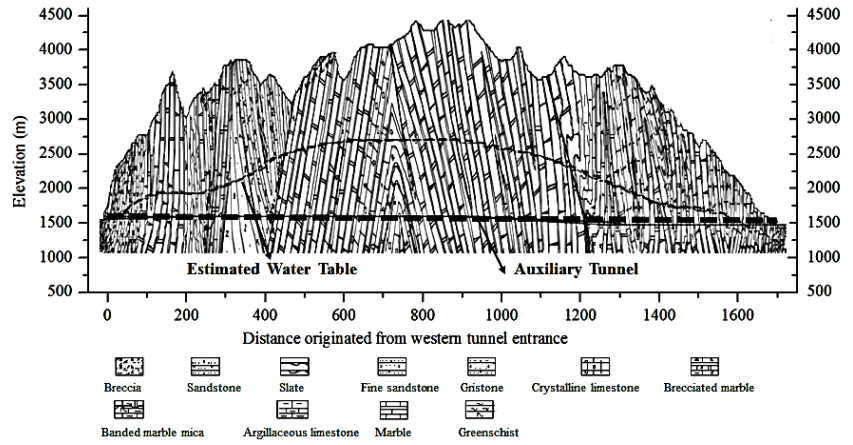

(a)

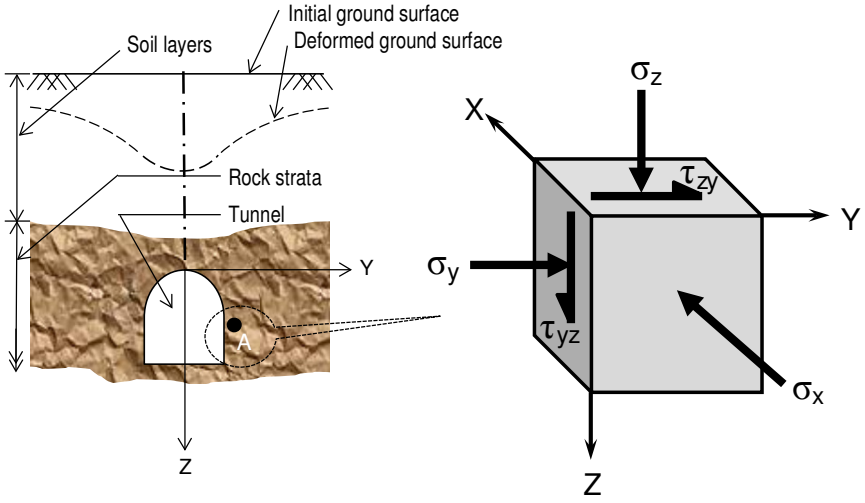

(b)

Figure 2: (a) Geological profile of the rock mass at the project site (modified after Zhou and Shan, 2013), and (b) Stress components on an element adjacent to tunnel surface

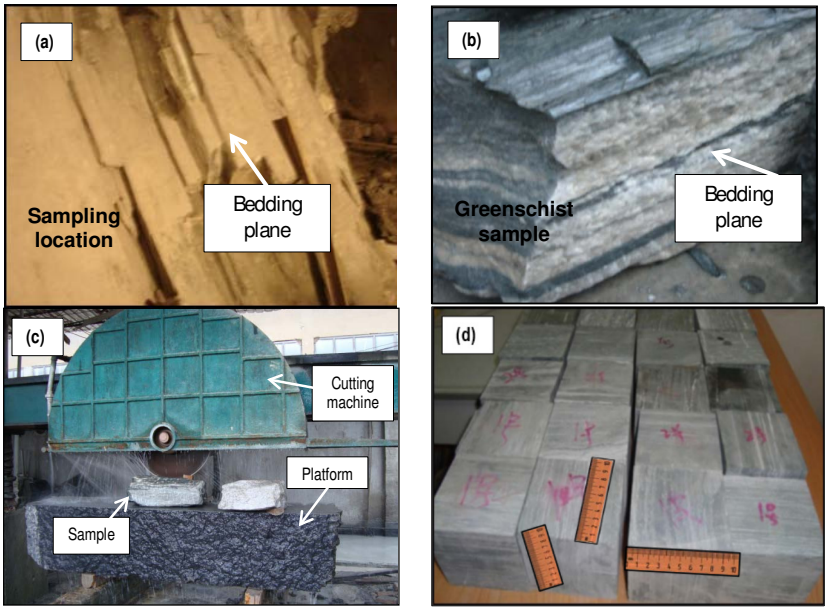

Figure 3: Rock sampling: (a) Chosen sample location, (b) Bedding plane location in Greenschist samle, (c) The rock cutting machine, and (d) Prepared samples.

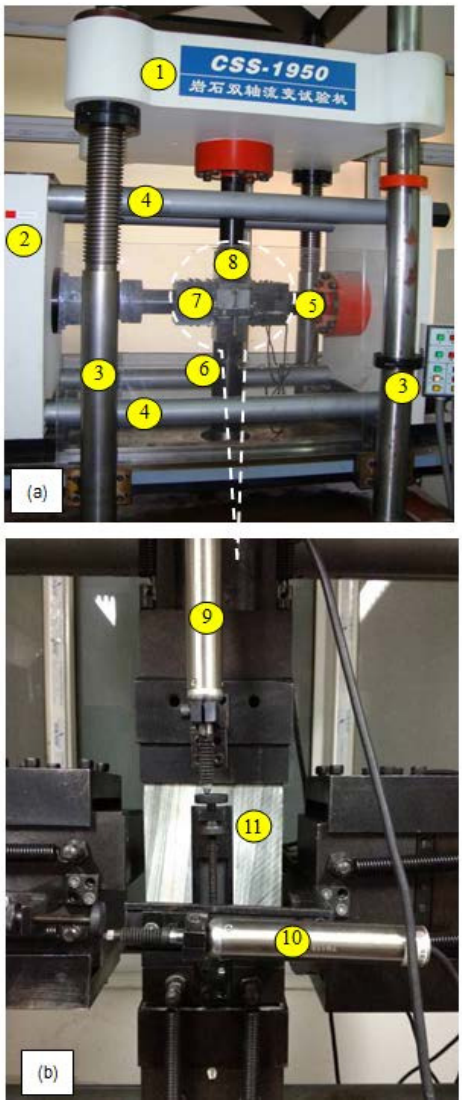

Legends: 1. Vertical support platform; 2. Horizontal support platform; 3. Vertical support rod; 4. Horizontal support rod; 5. Horizontal hydraulic rod; 6. Vertical hydraulic rod; 7. Horizontal Pressure Head; 8. Vertical Pressure Head; 9. Vertical LVDT; 10. Horizontal LVDT; 11. The rock specimen;

Figure 4 Rock biaxial rheological test machine (CSS–1950 type):
(a) Front view, and (b) Enlarged view of loading devices.

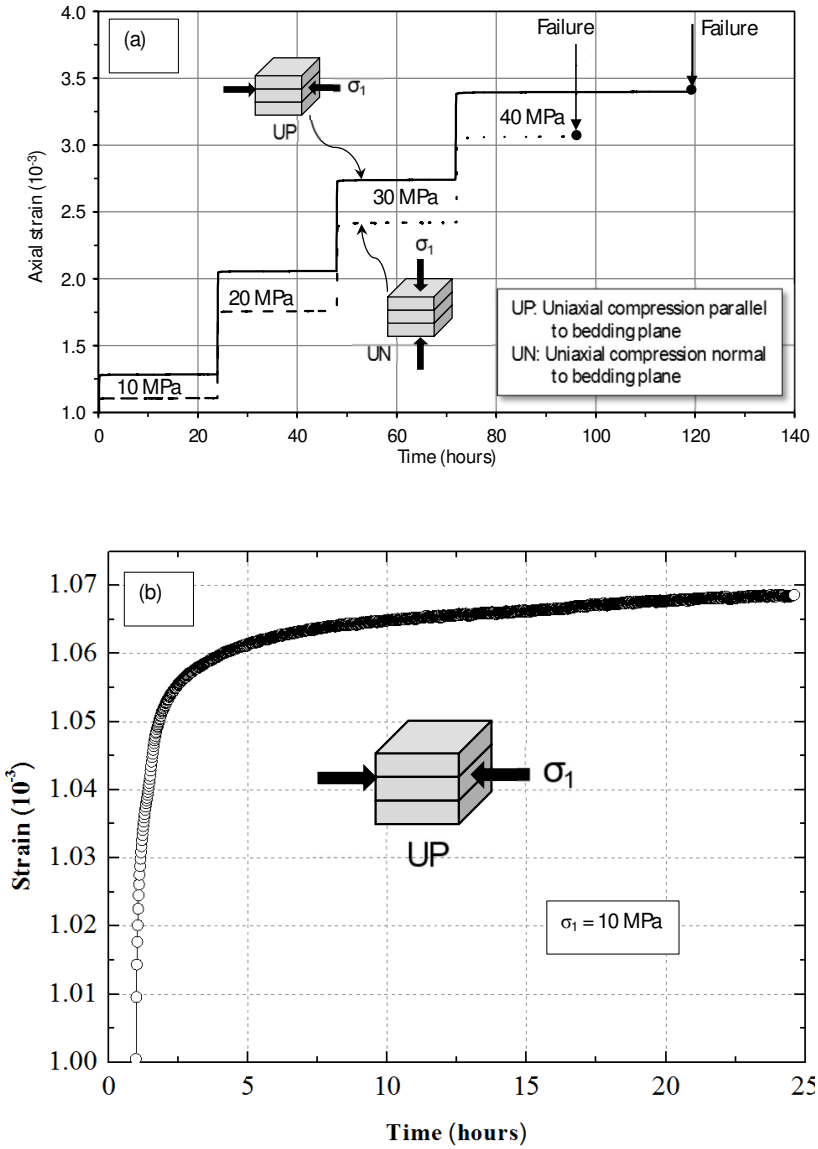

Figure 5: Uniaxial strain-time response: (a) Entire loading duration, and (b) The first stress step.

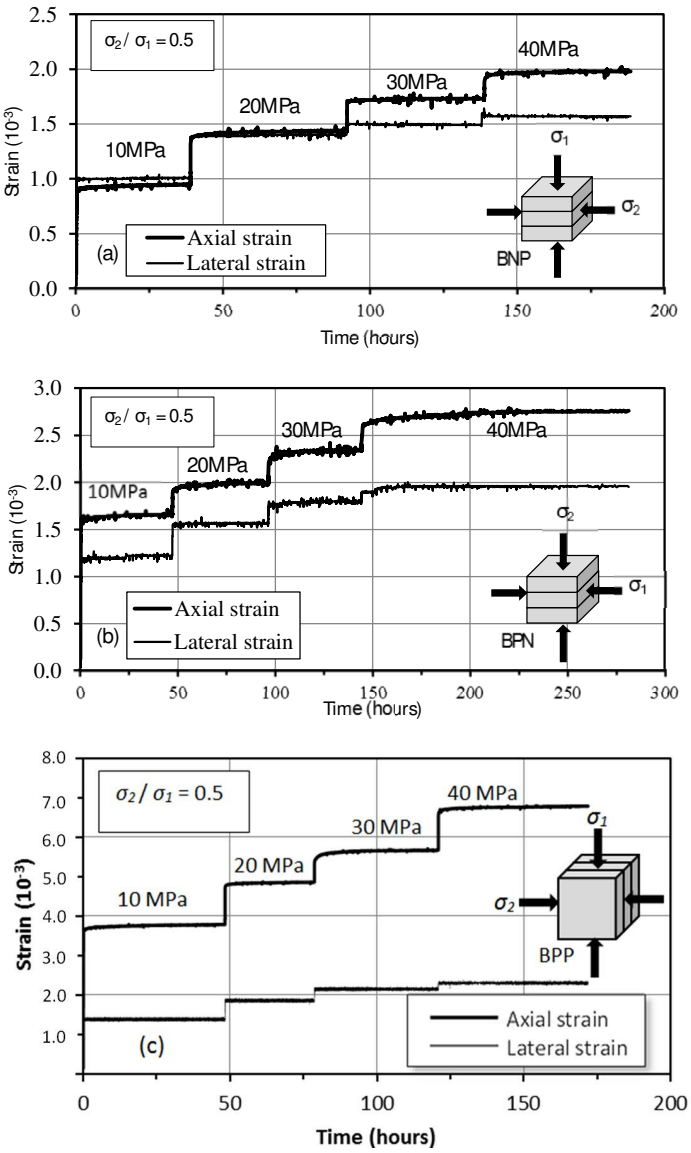

Figure 6: Biaxial strain-time response for: (a) BNP, (b) BPN, and (c) BPP.

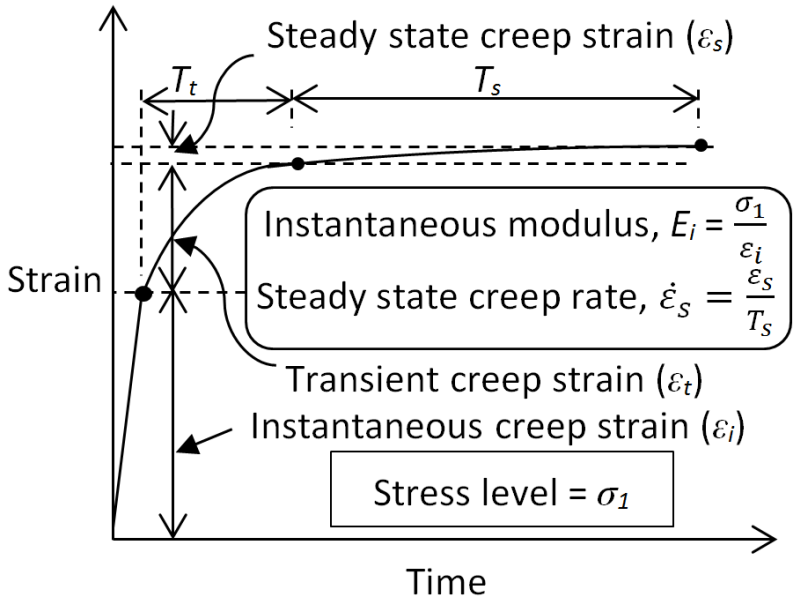

Figure 7: Definitions of various terms in relation to strain-time response.

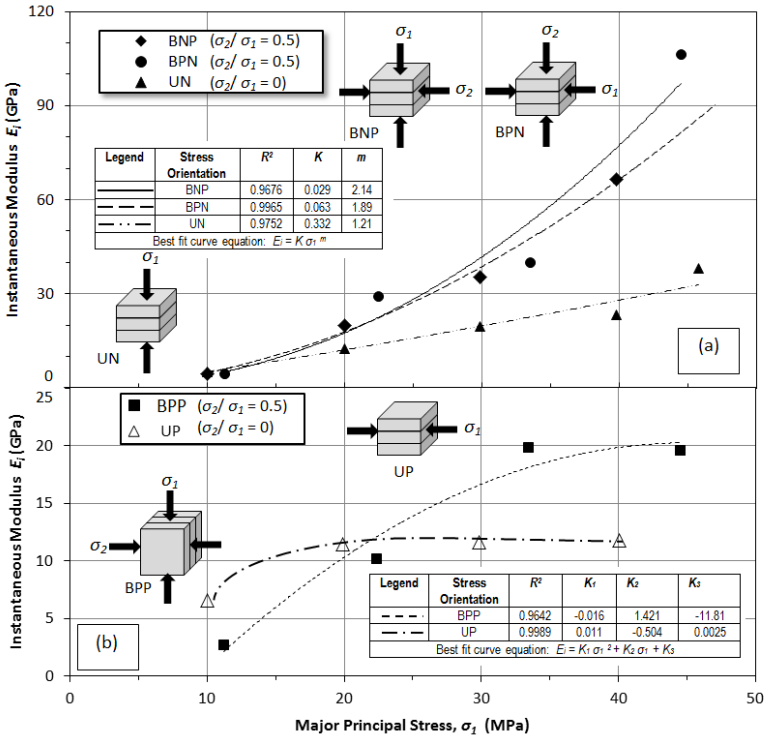

Legend	Stress Orientation	R^2	K	m
	BNP	0.9676	0.029	2.14
	BPN	0.9965	0.063	1.89
	UN	0.9752	0.332	1.21

Legend	Stress Orientation	R^2	K_1	K_2	K_3
	BPP	0.9642	-0.016	1.421	-11.81
	UP	0.9989	0.011	-0.504	0.0025

Figure 8: Variation of instantaneous modulus against major principal stress in case of:

(a) BNP, BPN & UN, and (b) BPP & UP.

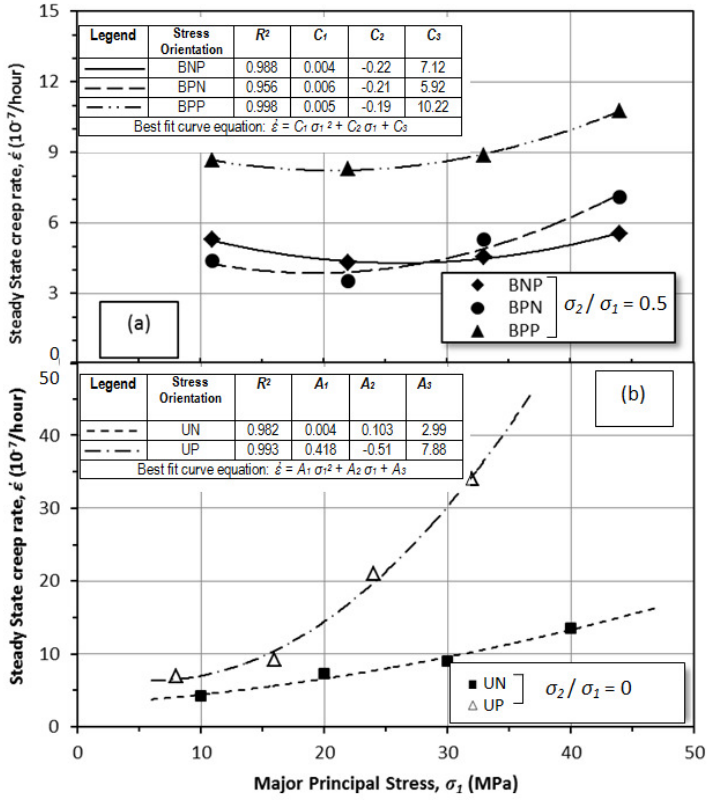

Figure 9: Variation of steady state creep rate against major principal stress in case of loading condition: (a) biaxial, and (b) uniaxial.

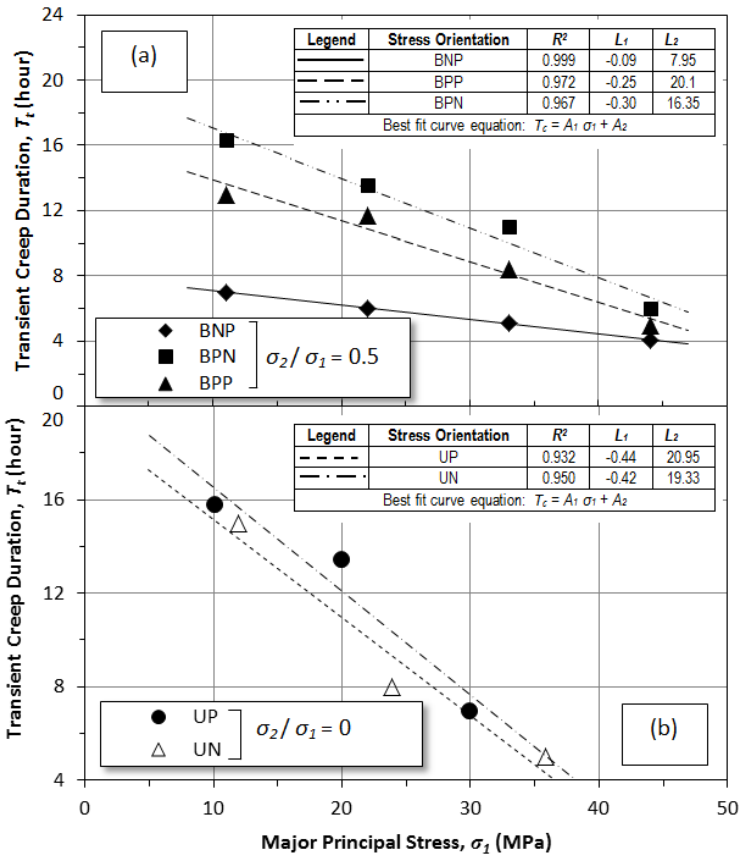

Figure 10: Variation of transient creep duration against major principal stress in case of loading condition: (a) biaxial, and (b) uniaxial.

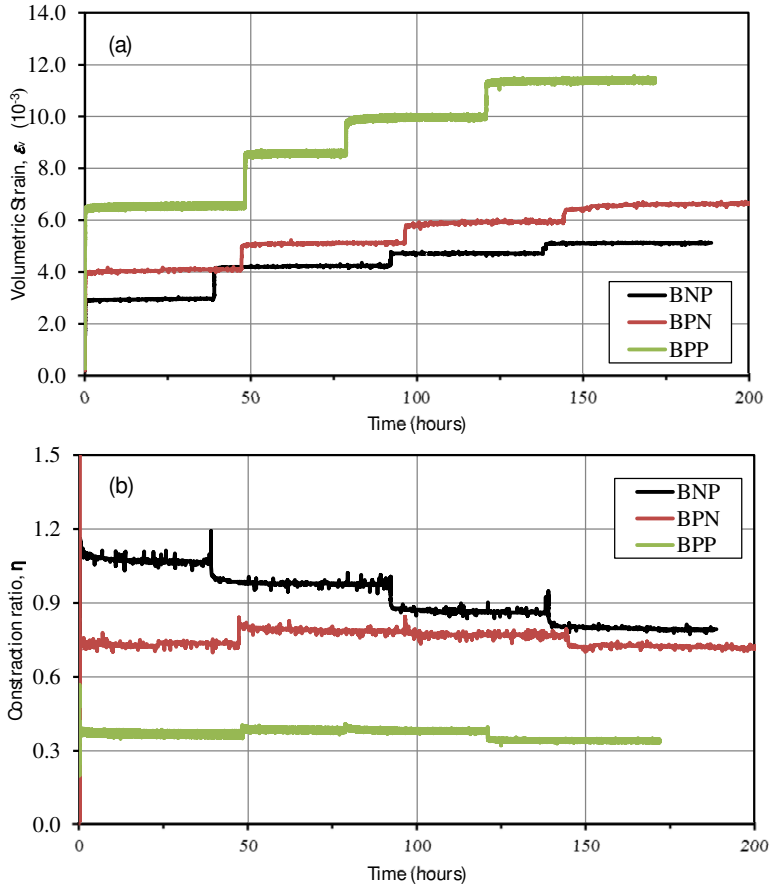

Figure 11: Time pattern of variation of: (a) volumetric strain, and (b) contraction ratio.